Optical design of the Chromospheric LAyer Spectro-Polarimeter (CLASP2)

Tsuzuki, Toshihiro, Ishikawa, Ryohko, Kano, Ryouhei, Narukage, Noriyuki, Song, Donguk, et al.

Toshihiro Tsuzuki, Ryohko Ishikawa, Ryouhei Kano, Noriyuki Narukage, Donguk Song, Masaki Yoshida, Fumihiro Uraguchi, Takenori J. Okamoto, David McKenzie, Ken Kobayashi, Laurel Rachmeler, Frederic Auchere, Javier Trujillo Bueno, "Optical design of the Chromospheric LAyer Spectro-Polarimeter (CLASP2)," Proc. SPIE 11444, Space Telescopes and Instrumentation 2020: Ultraviolet to Gamma Ray, 114446W (13 December 2020); doi: 10.1117/12.2562273

SPIE.

Event: SPIE Astronomical Telescopes + Instrumentation, 2020, Online Only

Optical design of the Chromospheric LAyer Spectro-Polarimeter (CLASP2)

Toshihiro Tsuzuki[a], Ryohko Ishikawa[a], Ryouhei Kano[a], Noriyuki Narukage[a], Donguk Song[a], Masaki Yoshida[b], Fumihiro Uraguchi[a], Takenori J. Okamoto[a], David McKenzie[c], Ken Kobayashi[c], Laurel Rachmeler[d], Frederic Auchere[e], Javier Trujillo Bueno[f], and CLASP2 team

[a]National Astronomical Observatory of Japan, 2-21-1 Osawa, Mitaka, Tokyo 181-8588, Japan
[b]Department of Astronomical Science, Graduate University for Advanced Studies (SOKENDAI), Tokyo 181-8585, Japan
[c]NASA Marshall Space Flight Center, Huntsville, AL 35812, USA
[d]NOAA National Centers for Environmental Information, Boulder, CO 80305, USA
[e]Institut d'Astrophysique Spatiale, CNRS/Univ. Paris-Sud 11, Batiment 121, 91405 Orsay, France
[f]Instituto de Astrofsica de Canarias, E-38205 La Laguna, Tenerife, Spain

ABSTRACT

Chromospheric LAyer Spectro-Polarimeter (CLASP2) was a sounding rocket experiment, which is a follow-up mission to the Chromospheric Lyman-Alpha Spectro-Polarimeter (CLASP1) in 2015. To measure the magnetic fields in the upper solar atmosphere in a highly quantitative manner, CLASP2 changes the target wavelengths from the hydrogen Ly-α line (121.567 nm) to Mg II lines near 280 nm. We reused the main structure and most of the optical components in the CLASP1 instrument, which reduced the turnaround time and cost. We added a magnifying optical system to maintain the wavelength resolution, even at the longer wavelength of CLASP2. Here, we describe the optical design and performance of the CLASP2 instrument.

Keywords: CLASP1, CLASP2, Sounding rocket experiment, Spectro-Polarimeter, UV lines

1. INTRODUCTION

The chromospheric and coronal heating mechanism and the solar wind acceleration mechanism remain unresolved in solar physics. The magnetic fields are believed to play a critical role in these mechanisms. Accurate magnetic field measurements in the chromosphere and transition region, which are the interfacial layers between the solar surface (photosphere) and the corona, are critically important for understanding these mechanisms. However, information on the magnetic field in these layers is greatly lacking.

The solar magnetic field is measured by observing the polarization signals induced in spectral lines. In the ultraviolet (UV) light originating in the upper chromosphere and higher, there are two candidates whose polarization signals are theoretically predicted to be measurable[1] : the hydrogen Ly-α line at 121.567 nm[2] and the Mg II h- and k-lines around 280 nm.[3] First, focusing on the Ly-α line, our international team performed Chromospheric Lyman-Alpha Spectro-Polarimeter[4] (CLASP1). The CLASP1 instrument (Fig. 1) was used to measure the intensity and linear polarization spectra at the Ly-α line,[5–12] and launched with a NASA sounding rocket from the White Sands Missile Range (WSMR) in September 2015. As a result of the 5-minute observation, we achieved (1) unprecedented high polarization accuracy and precision of 0.1% in vacuum UV,[13,14] (2) the acquisition of scattering polarization from the upper chromosphere and the transition region,[15] and (3) the detection of the Hanle effect[16] (modification of the scattering polarization induced by the presence of the magnetic field[17]). CLASP1 therefor opened up a new way of performing UV spectropolarimetry in solar physics. However, the observation data also suggest that the scattering polarization in these upper layers is much more complicated

Further author information: (Send correspondence to T.T.)
T.T.: E-mail: toshihiro.tsuzuki@nao.ac.jp, Telephone: +91 422 34 3891

Space Telescopes and Instrumentation 2020: Ultraviolet to Gamma Ray, edited by Jan-Willem A. den Herder Shouleh Nikzad, Kazuhiro Nakazawa, Proc. of SPIE Vol. 11444, 114446W · © 2020 SPIE
CCC code: 0277-786X/20/$21 · doi: 10.1117/12.2562273

than expected from state-of-art 3D atmospheric models,[18,19] leading to the difficulty of qualitative measurement of the magnetic field without refining the model. To overcome this difficulty, we proposed a new sounding rocket experiment Chromospheric LAyer Spectro-Polarimeter[20] (CLASP2).

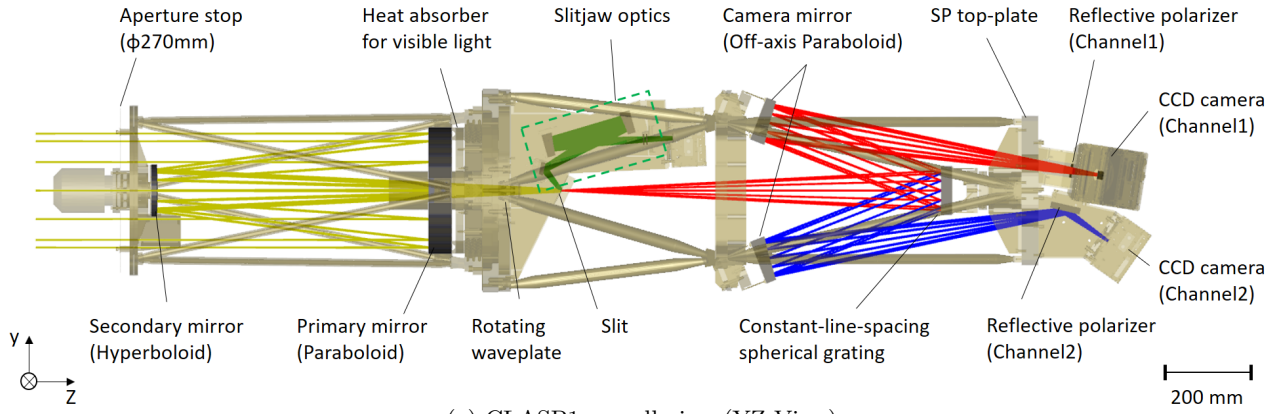

(a) CLASP1 overall view (YZ View)

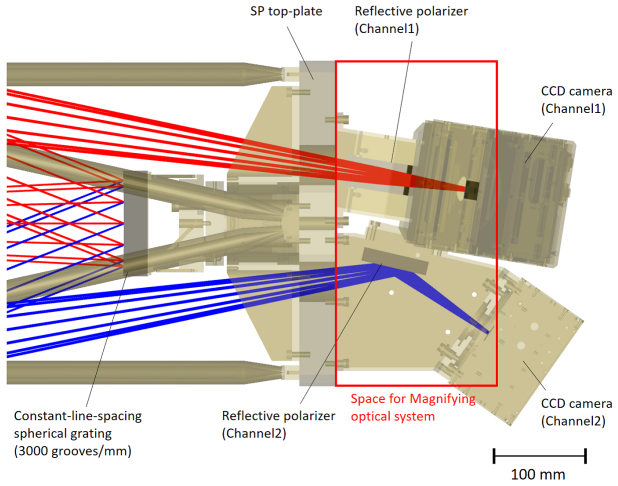

(b) Enlarged view (YZ View)

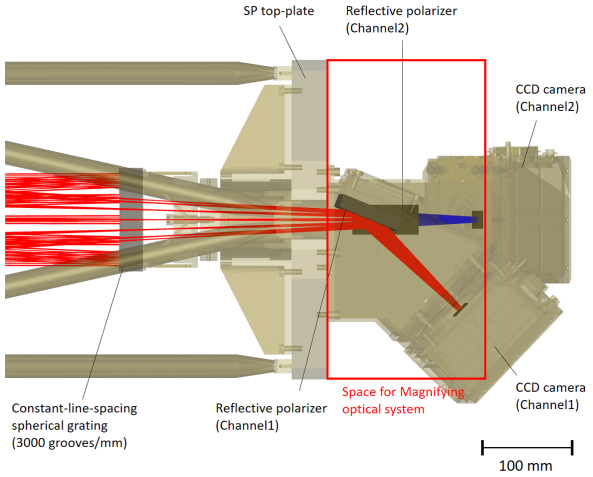

(c) Enlarged view (XZ View)

Figure 1: Structural model and optical path diagram of CLASP1. The red rectangle indicates the area that can be used for the magnifying optical system. The colored rays represent the following: (yellow) Telescope, (green) slit-jaw Optics, (red) spectrograph(channel1), (blue) spectrograph(channel2)

The targeted spectral lines of CLASP2 are the Mg II h- and k-lines near 280 nm. The advantage of these spectral lines is that the circular polarization induced by the Zeeman effect can be measured in a strongly magnetized region of >50 G, as well as the linear polarization caused by the scattering and the Hanle effect.[21,22] The Zeeman diagnostic has been widely used (e.g., the Hinode satellite), and the interpretation is much more straightforward than the Hanle effect because circular polarization signals appear depending on the strength of the longitudinal components of the magnetic field. The quantitative information provided by the circular polarization will help us interpret the linear polarization (i.e., estimate the degree of the Hanle effect) and uniquely determine the vector magnetic field.[23] Thus, we aim to measure the intensity, linear, and circular polarization spectra in the Mg II h- and k-lines around 280 nm by refitting the CLASP1 instrument. Our requirements for the wavelength resolution and polarization accuracy are 0.01 nm and 0.1%, respectively, which are the same as those for CLASP1.

The CLASP1 instrument returned to the ground without any damage after the first flight, and we confirmed with our optical tests that the optical alignment was still intact and ready for a re-flight. The cost and turnaround

time were minimized by reusing the structure and optical components as much as possible from CLASP1, without compromising the requirements. We herein describe the optical design of CLASP2 in detail.

2. PRINCIPLE OF OPTICAL SYSTEM CHANGE

In CLASP2, the optical system was modified to accommodate the Mg II lines (280 nm) from that in CLASP1, which was optimized for the Ly-α line (121.567 nm). The policy for changing the optical components of CLASP1 to CLASP2 is described below.

2.1 Telescope

The telescope of CLASP1 is a Cassegrain type and is used to image the sun on the slit mirror. In CLASP2, both the optical elements and structure of the telescope are reused without change. However, the cold-mirror coating on the primary mirror, to eliminate the visible light to the subsequent optical components is changed to one optimized for two wavelength regions: Mg II lines for the spectro-polarimeter (SP) and the Ly-α line (121.567 nm) for the slit-jaw optical system.[24]

2.2 Slit-jaw Optical system

The functions of the slit-jaw optical system[25] are (1) to confirm and adjust the pointing during flight, (2) to provide the context chromospheric images for the co-alignment with other satellites and ground-based telescopes and for the interpretation of the spectropolarimetric data. Because these functions are sufficiently accomplished by the CLASP1 slit-jaw optical system, which takes the Ly-α line, the slit-jaw optical system is not modified.

2.3 Spectrograph

The CLASP1 spectrograph[5] is an inverse Wadsworth mounting type, which consists of a slit, a spherical grating, two off-axis parabolic mirrors, and two CCDs. A spherical grating diffracts the diverging light from the slit into the $\pm$1st-order quasi-parallel light symmetrically. Then, an off-axis parabolic mirror ("camera mirror") in each quasi-parallel light makes dispersed slit images on a CCD sensor. With these two optically symmetrical channels, the two orthogonal polarization states are measured simultaneously to significantly suppress the spurious polarization to less than 0.1%, caused by the change in the solar intensity and drift and jitter of the rocket. In CLASP2, the observation wavelength is changed from 121.567 to 280 nm, though the arrangement of the optical elements up to the camera mirror remains the same as in CLASP1. Therefore, the radius of curvature of the CLASP2 spherical grating is kept as that of CLASP1, while the groove density of the CLASP2 spherical grating is changed such that the diffraction angle at 280 nm is the same as that of the Ly-α line of CLASP1 (121.567 nm). However, this change alone results in the degradation of the wavelength resolution because the wavelength resolution is inversely proportional to the observation wavelength. Therefore, to maintain the same wavelength sampling as CLASP1, we include a magnifying optical system downstream of the camera mirror to double the f-number of the spectrograph. Furthermore, the magnifying optical system must improve the image quality so that the RMS spot diameter is kept within 26 μm (equivalent to a wavelength of 0.01 nm). The slit width is also changed to 7 μm, which is half of the CLASP1's to match it to the CCD pixel size of 13 μm. To do so, the wavelength resolution is maintained at 0.01 nm and the spatial resolution can be improved to 1.1 arcseconds, which is half that of CLASP1. The optical design of the magnifying optical system is described in the next section.

2.4 Polarimeter Optics

A polarimeter optical system consists of a rotating waveplate[6,9] and polarization analyzers. In CLASP1, only reflective polarizers are available because most of the materials absorb the Ly-α lights. In contrast, wire-grid-type transmissive polarizers[26] are available at a wavelength near 280 nm and are used in CLASP2. The principal axis of the two polarizers is placed parallel and perpendicular to the ruling direction of the grating in order to measure two orthogonal polarizations simultaneously.

3. DESIGN OF MAGNIFYING OPTICAL SYSTEM

3.1 Specifications of the magnifying optical system

The optical design specifications of the newly added magnifying optical system are summarized in Tab. 1. The main structure, optical path of CLASP1, and available space for the magnifying optical system are shown in Fig. 1. As shown, to reuse the CLASP1 rocket skin, the additional magnifying optical system must fit into the limited space in the rear stage.

Table 1: Design specifications for additional magnifying optical system of CLAPS2. The positions of SP top-plate and CLASP1 CCDs are shown in Fig. 1.

Items	**Specifications**
Wavelength (in vacuum)	279.64 nm (Mg II k-line), 280.35 nm (Mg II h-line)
FoV (Field of view)	200 arcsec
Plate scale	0.005 nm/pixel (13 μm/pixel)
Image quality	RMS spot radius including former optical system should be less than 13 μm as built performance.
Optical elements	The following optical elements should be positioned to a downstream side of SP top-plate. (See Fig. 1)
(1) Transmissive Polarizer	Made of Fused silica. The dimensions are 50 mm x 50 mm x 1 mm
(2) ND filter	Made of Fused silica. The thickness is 2 mm.
(3) Fold mirrors	few fold mirrors are available to fit the optical system into the rockets skin.
(4) CCD camera	Z position of the CLASP2 CCD camera should be in front of that of CLASP1. The X and Y positions can move several mm compared to the CLASP1 CCD camera position.

3.2 Design policy of the magnifying optical system

Based on the design specifications described in the previous section, we established the following three design policies for the magnifying optical system.

1) Power arrangement
The magnifying optical system is located at the back of CLASP1 as an additional optical system to enlarge the image of CLASP1 by a factor of two and reimage it at approximately the same position. The power of the magnifying optical system should be negative. For the mirror to generate negative power, a hyperboloid convex mirror seems to be the best choice because real images need to be created from virtual images.

2) Improvement in image quality
The residual aberrations of the former optical system (i.e. from the aperture to the camera mirror) are so large that the overall optical system using only an ideal magnifier does not meet the image quality specifications (13 μm RMS spot radius) as shown in Fig. 2. Both the spherical aberration caused by a spherical grating and the off-axis aberrations at the edge of the FoV are significant for the image quality of the entire optical system. Because of the minimal ability in the downstream of the optical system to correct spherical aberrations, the additional optical system should correct the residual aberrations, especially the off-axis aberrations seen at the edge of the FoV. To eliminate coma and astigmatism with a small number of optical elements, asymmetric optical elements such as wedge prisms and off-axis mirrors are effective. In addition, because of the extremely limited area in the rocket skin, it is necessary to fold the optical path. However, the additional fold mirrors should be as limited as possible because they affect wavefront error, as-built performance, throughput, alignment effort, and cost.

3) Symmetrical system
Unlike CLASP1, two channels can be positioned symmetrically with the XZ plane because of the availability

of transmissive polarizers in CLASP2. This indicates that the magnifying optical system for each channel can be the same and is positioned symmetrically with the XZ plane.

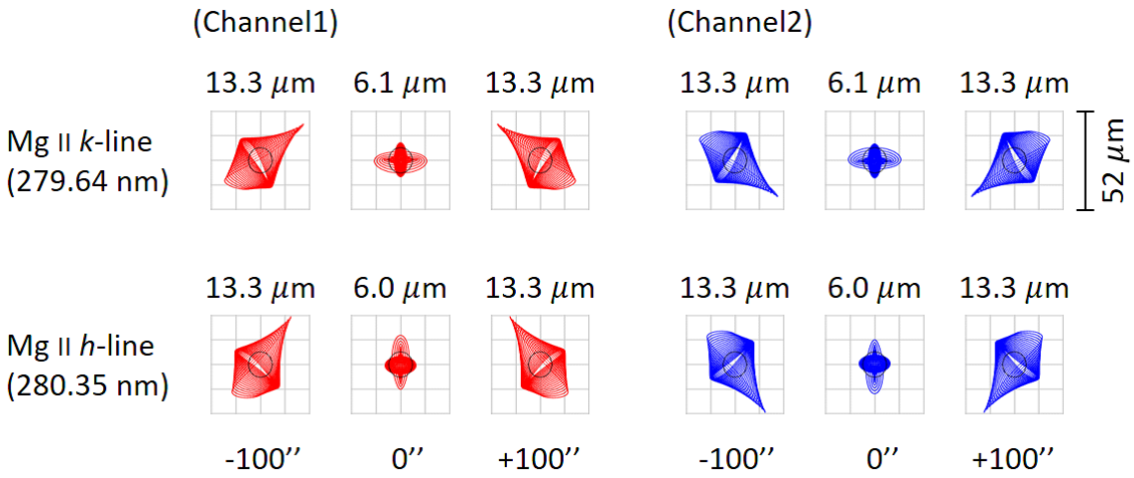

Figure 2: Spot diagrams of CLASP1 combined with a paraxial lens as the magnifying optical system. The horizontal direction is the slit direction (field of view) and the vertical direction shows two observation wavelengths (Mg II k and Mg II h). The numbers at the top indicate the RMS spot radius and the black circles at the center represent an airy disk. The size of the diagram is 52 μm (equivalent to 4 pixels), which corresponds to 2.2 arcsecond in space and 0.02 nm in wavelength.

3.3 Design detail and nominal performance

In the design process, we first proposed several optical design types that can meet the specifications based on the policies described in Sec. 3.2. Then, considering the image quality, ease of handling, and other factors, we selected the following two candidates.

Type A lens optical system with a wedge prism as negative power (Fig. 3a)

Type B all-reflective optical system using an off-axis hyperboloid mirror as negative power (Fig. 3b)

Regarding the nominal image quality, Type A was better than Type B. Regarding the number of optical elements, Type A requires four elements (a wedge, a lens, and two fold mirrors), whereas Type B requires two elements (a hyperboloid mirror and a fold mirror) to fit within the limited area. A tolerance analysis shows that Type B has a better as-built performance, mainly because it has fewer elements and surfaces. From of alignment perspective, Type B is superior to Type A because it can be aligned and tested in air. The transmissive optical elements in Type A make a significant change in the image quality between air and vacuum. Considering these results and cost estimation, we selected Type B (i.e., all-reflective optical system) as the best solution. The final optical layout is shown in Fig. 4. The entire optical system has symmetry with the YZ plane, and the two channels are symmetrical with the XZ plane. The magnifying optical system is contained in a limited space with only one flat mirror.

The imaging performance of the CLASP2 overall optical system is shown in Fig. 5. Compared to the image quality of CLASP1 with paraxial lenses (Fig. 2), the performance at the edge of the FoV is improved and the worst value of the RMS spot radius over the FoV improves by approximately half. The RMS spot radius of the design is less than 6.6 μm, which meets the image quality specifications (13 μm).

The changes in the optical parameters from CLASP1 are summarized in Tab. 2.

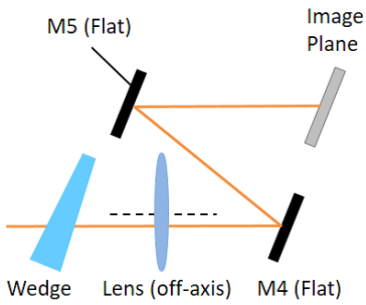

(a) Type A

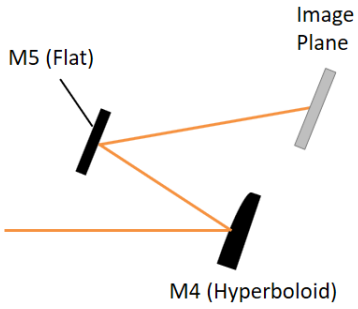

(b) Type B

Figure 3: Schematic layout of two candidates for the magnifying optical system. (a) Type A: Lens optical system with a wedge prism as negative power. (b) Type B: All-reflective optical system using a hyperbolic mirror as negative power. Note that planar transmittance elements (transmission polarizers and ND filters) are not shown in this figure.

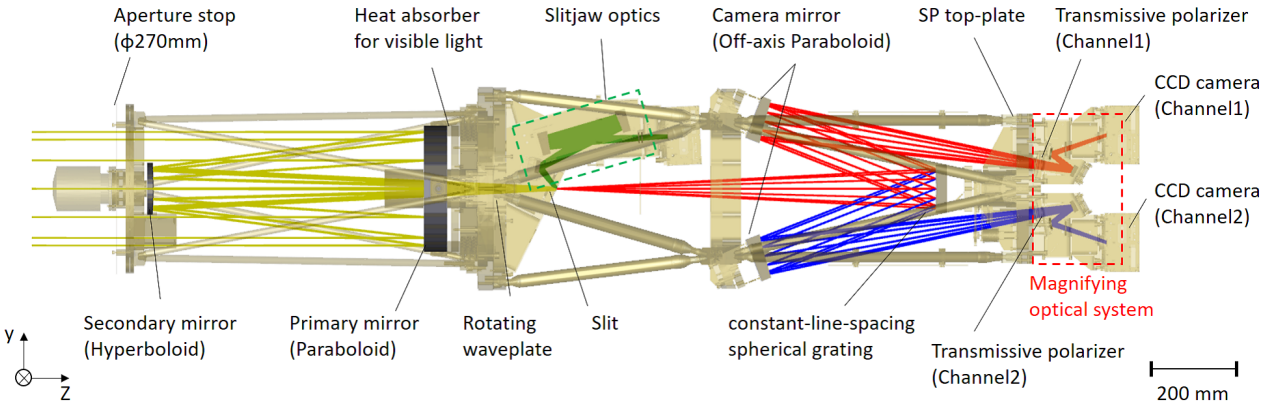

(a) CLASP2 overall view (YZ View)

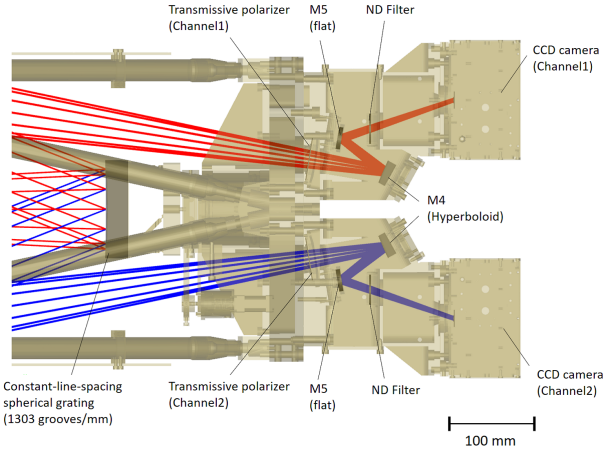

(b) Enlarged view (YZ View)

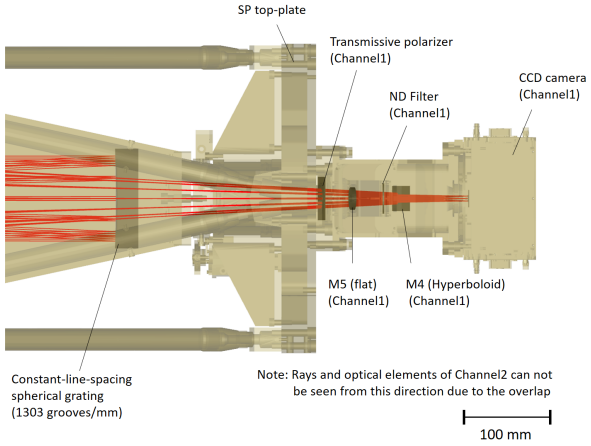

(c) Enlarged view (YZ View)

Figure 4: Structural model and optical path layout of CLASP2. The groove density of the grating is changed so that the same optical path is taken at the wavelength of 280 nm in CLASP2 as at the Ly-α line in CLASP1. The magnifying optical system consists of one hyperboloid mirror and one fold mirror to achieve the required functions within the limited space. The two channels are symmetrical in the XZ plane. The colors of the rays of light are the same as those in Fig. 1.

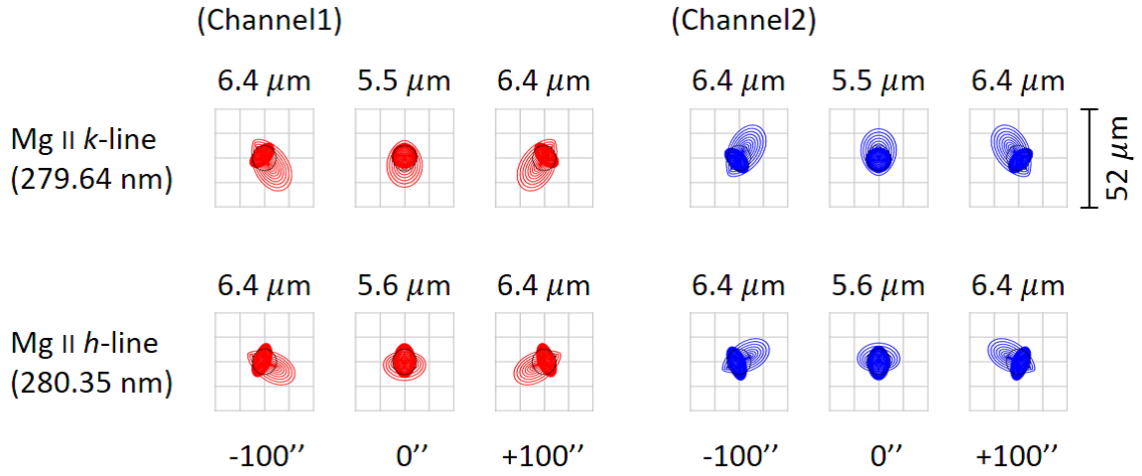

Figure 5: Same as Fig. 2 but for CLASP2. The performance at the edge of the FoV is improved compared to the CLASP1 imaging performance (Fig. 2) .

Table 2: Changes in optical parameters of CLASP2 from CLASP1 optical system.

Item		**CLASP1**[5]	**CLASP2**
System Parameter			
Wavelength		121.567 nm	279.55, 280.27 nm
Final F number		9.42	18.9
Plate-scale	Spectral	0.0048 nm/pixel	0.0050 nm/pixel
	Spatial	1.11 arcsec/pixel	0.55 arcsec/pixel
Resolution	Spectral	0.010 nm	0.010 nm
	Spatial	3.0 arcsec	1.1 arcsec
Telescope			
Primary Mirror	Coating	Cold mirror coating optimised for Lyα-line	Cold mirror coating optimised for Lyα and Mg II lines
Spectropolarimeter			
Slit	Slit width	18.4 μm (1.45 arcsec)	7 μm (0.55 arcsec)
	Slit length	5.1 mm (400 arcsec)	2.5 mm (200 arcsec)
Grating	Groove density	3000 lines/mm	1303 lines/mm
Camera Mirror	Distance to next	827.5 mm (to CCD)	108.05 mm (to M4)
Polarizer		Reflective type	Transmissive type (1 mm thickness, Fused Silica)
Magnification optical system			
Magnification power		N/A	2
M4	Surface figure	N/A	Hyperboloid (K = -6.778)
	Off-axis value	N/A	34.44 mm
	Curvature radius	N/A	341.19 mm
	Distance to next	N/A	73.22 mm (to M5)
M5	Surface figure	N/A	Flat
	Distance to next	N/A	138.75 mm (to CCD)
ND Filter		None	Absorptive type (2 mm thickness, Fused Silica)

3.4 Tolerance analysis and error budget plan

In order to evaluate the performance, including acceptable errors in assembly and manufacturing as well as to determine the compensators in alignment and their stoke, we conducted tolerance analyses of the spectropolarimeter (i.e., grating, camera mirror and the magnifying optical system). With the feasible tolerance, we found that three compensators (i.e., CCD defocus, M4 X-tilt, and M4 Y-tilt) are needed to meet the image quality specifications, and the other three compensators (i.e., M5 X-tilt, Y-tilt, and Z-shift) are needed to compensate the image shifts. The results of a Monte Carlo analysis assuming parabolic tolerance distributions (N = 10000) are shown in Fig. 6a. The error budget plan for imaging performance is also shown in Fig. 6b . Here, we assume that the adjustment errors are 20 μm in the CCD defocus and 2 arcmin in M4 X/Y-tilt and that errors due to the fore optical system consist of a telescope-axis misalignment and a slit position misalignment. It is expected that the assembled instrument satisfies the specification of the image quality (13 μm) in the RMS spot radius).

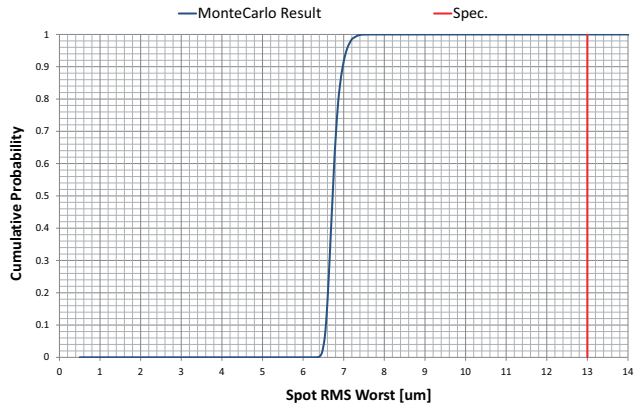

(a) Monte Carlo analysis result

Error factor	RMS Spot Radius [um]
Nominal performance	6.4
Fabrication + Install (3σ)	3.6
Adjustment error	1.9
Fore Optics error	
Telescope axis error	2.1
Slit position error	3.5
Root sum square	8.6

(b) RMS spot radius error budget plan

Figure 6: (a) Monte Carlo analysis result and (b) the error budget plan for RMS spot radius. The Monte Carlo simulation consists of 10,000 trials. We assumed a parabolic distribution in each error, and assumed an adjustment using three comparators. The cumulative probability (3σ) is 7.4 μm, which is well below the specification (13 μm). The total RSS value of the RMS spot radii is 8.6 μm, which also shows that the design satisfies the specification.

3.5 Stray light effect

Because the CLASP2 instrument uses a part of the CLASP1 instrument, two types of stray light were considered: (1) stray light recognized in the CLASP1 instrument and (2) stray light owing to the magnifying optical system added to CLASP2. In CLASP1, although no serious problems were expected in the stray light analysis on a ray-trace-based analysis software, during the Sun test, we recognized that the diffracted light by the slit passed through the side of the grating and reached the CCDs. To suppress the stray light, we changed the size of the baffle located between the slit and the grating and added new baffles besides the grating, and confirmed in the second Sun test that the amount of CLASP1 stray light reduced to approximately 0.8% of the Ly-α signal. A possible source of stray light in the magnifying optical system is the multiple reflection from the ND filter placed in front of the CCDs (see Fig. 4b). Because of the inclined incidence, the double reflection by the filter makes an image at the location shifted by 0.893 mm, which corresponds to about half of the distance between the Mg II k-lines. However, such an image is significantly (10 times) blurred. Therefore, the effect of the double reflection is just 1% of the signal even without the AR coating. From these results, we conclude that the effect of the double path has an insignificant effect on the observation even if ND filters are uncoated.

4. SUMMARY AND CURRENT STATUS OF CLASP2

We modified the optical system of CLASP1 designed for the hydrogen Ly-α line (121.567 nm) to accommodate Mg II lines (280 nm). After considering several optical types, the best design solution that meets the specifications was

presented. The new CLASP2 optical system has a more symmetric design and better image quality than CLASP1. In addition, a tolerance analysis and error budget plan demonstrated the feasibility of this solution. Following this CLASP2 optical design, the optical elements were manufactured and then mounted to the structure. After the optical alignment, the image quality of the CLASP2 SP was confirmed to satisfy the requirements (RMS spot radius of 13 μm) anywhere on the slit[27] (see Appendix A). Therefore, we conclude that our strategy for the CLASP2 optical design demonstrated here is appropriate. Note that CLASP2 was launched on April 11, 2019 in WSMR, NM, U.S.A. and succeeded in the spectropolarimetric observation around Mg II h- and k-lines. It is expected that many discoveries will be made based on this data in the future.

APPENDIX A. COMPARISON BETWEEN DESIGNED AND MEASURED SPOT IMAGES

The optical alignment of CLASP2 SP was performed in 2018, as in the previous SPIE conference.[27] Fig. 7 shows the pinhole images simulated by using the designed point-spread-functions and the measured pinhole images after the alignment. Although the actual pinhole images are slightly larger than the simulated ones, they satisfy our requirements (the RMS spot radius is 13 μm) anywhere on the slit.

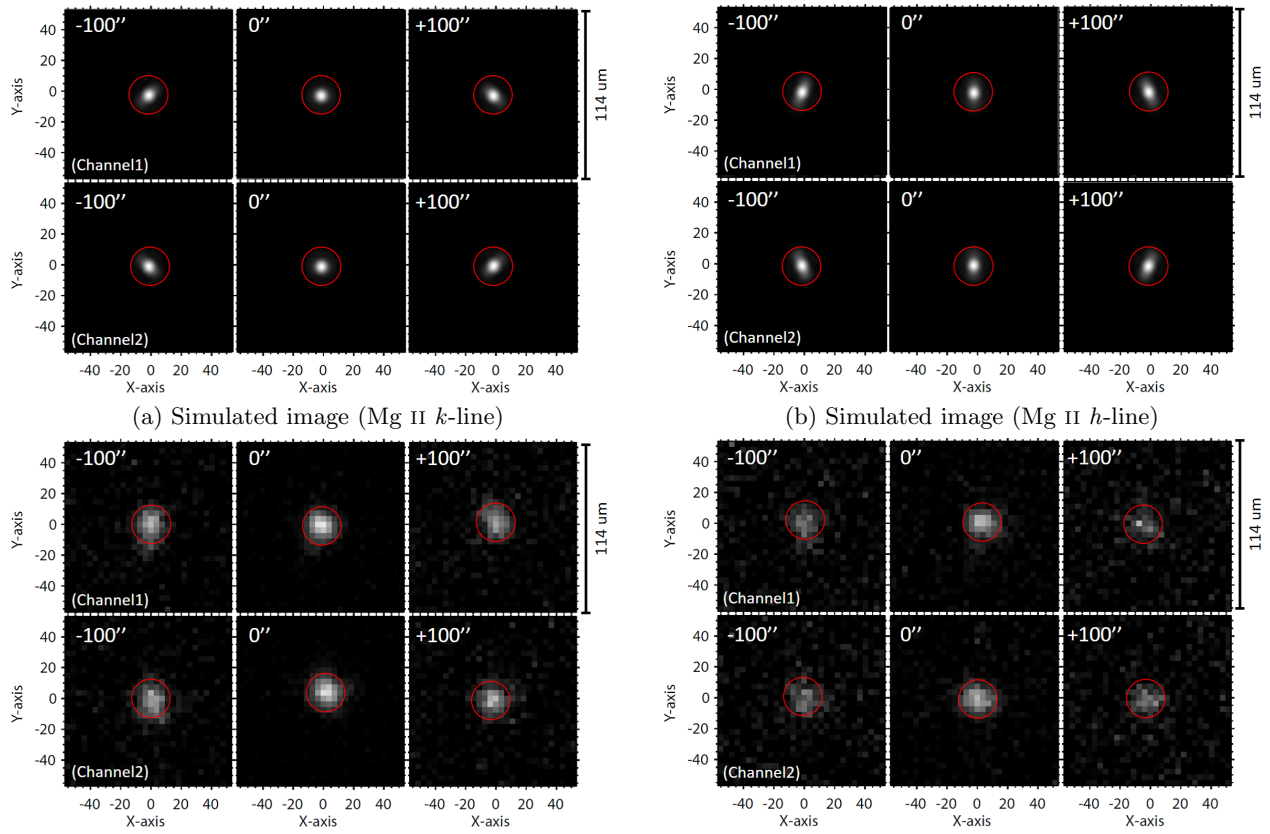

(a) Simulated image (Mg II k-line)

(b) Simulated image (Mg II h-line)

(c) Measured image (Mg II k-line)

(d) Measured image (Mg II h-line)

Figure 7: Comparison between the simulated pinhole images by using PSFs of optical design and the measured pinhole images after alignment in the Mg II k- and h-lines. The actual pinhole images were taken by a GSE camera whose pixel size is 3.8 μm, because the flight CCD camera has too large pixel size (13 μm) to evaluate the image quality.[27] The plot area is 114 μm, which is equivalent to 30 pixels in the flight camera. The red circle represents our requirements (RMS spot radius of 13 μm).

ACKNOWLEDGMENTS

We greatly appreciate the Chromospheric Lyman-Alpha Spectro-Polarimeter (CLASP1) team and the Chromospheric LAyer Spectro-Polarimeter (CLASP2) team. CLASP2 is an international partnership between NASA Marshall Space Flight Center (NASA/MSFC), National Astronomical Observatory of Japan (NAOJ), Japan Aerospace Exploration Agency (JAXA), Institut d'Astrophysique Spatiale (IAS), and Instituto de Astrofísica de Canarias (IAC); additional partners include Academy of Sciences of the Czech Republic (ASCR), Istituto Ricerche Solari Locarno (IRSOL), Lockheed Martin Solar & Astrophysics Laboratory (LMSAL) and the University of Oslo. The Japanese participation is funded by JAXA as a Small Mission-of-Opportunity Program, by JSPS KAKENHI Grant numbers JP25220703 and 16H03963, 2015 ISAS Grant for Promoting International Mission Collaboration, and 2016 NAOJ Grant for Development Collaboration. The US participation is funded by NASA Award 16-HTIDS16_2-0027. The French hardware participation is funded by Centre National d'Etudes Spatiales (CNES) funds CLASP2-13616A and 13617A. The Spanish participation is funded by the European Research Council (ERC) under the European Union's Horizon 2020 research and innovation programme (ERC Advanced Grant agreement No 742265).

REFERENCES

[1] Trujillo Bueno, J., Landi Degl'Innocenti, E., and Belluzzi, L., "The Physics and Diagnostic Potential of Ultraviolet Spectropolarimetry," *Space Sci. Rev.* **210**, 183–226 (Sept. 2017).

[2] Trujillo Bueno, J., Štěpán, J., and Casini, R., "The Hanle Effect of the Hydrogen Lyα Line for Probing the Magnetism of the Solar Transition Region," *Astrophys. J.* **738**, L11 (Sep 2011).

[3] Belluzzi, L. and Trujillo Bueno, J., "The Polarization of the Solar Mg II h and k Lines," *Astrophys. J.* **750**, L11 (May 2012).

[4] Kano, R., Bando, T., Narukage, N., Ishikawa, R., Tsuneta, S., Katsukawa, Y., Kubo, M., Ishikawa, S.-n., Hara, H., Shimizu, T., Suematsu, Y., Ichimoto, K., Sakao, T., Goto, M., Kato, Y., Imada, S., Kobayashi, K., Holloway, T., Winebarger, A., Cirtain, J., De Pontieu, B., Casini, R., Trujillo Bueno, J., Štepán, J., Manso Sainz, R., Belluzzi, L., Asensio Ramos, A., Auchère, F., and Carlsson, M., "Chromospheric Lyman-alpha spectro-polarimeter (CLASP)," *Proc. SPIE* **8443**, 84434F (Sept. 2012).

[5] Narukage, N., Auchère, F., Ishikawa, R., Kano, R., Tsuneta, S., Winebarger, A. R., and Kobayashi, K., "Vacuum ultraviolet spectropolarimeter design for precise polarization measurements," *Applied Optics* **54**, 2080 (Mar 2015).

[6] Ishikawa, R., Kano, R., Bando, T., Suematsu, Y., Ishikawa, S.-n., Kubo, M., Narukage, N., Hara, H., Tsuneta, S., Watanabe, H., Ichimoto, K., Aoki, K., and Miyagawa, K., "Birefringence of magnesium fluoride in the vacuum ultraviolet and application to a half-waveplate," *Applied Optics* **52**, 8205 (Dec 2013).

[7] Ishikawa, R., Narukage, N., Kubo, M., Ishikawa, S., Kano, R., and Tsuneta, S., "Strategy for Realizing High-Precision VUV Spectro-Polarimeter," *Sol. Phys.* **289**, 4727–4747 (Dec 2014).

[8] Giono, G., Ishikawa, R., Katsukawa, Y., Bando, T., Kano, R., Suematsu, Y., Narukage, N., Sakao, T., Kobayashi, K., and Auchère, F., "Current progress of optical alignment procedure of CLASP's Lyman-alpha polarimetry instrument," *Proc. SPIE* **9144**, 91443E (July 2014).

[9] Ishikawa, S., Shimizu, T., Kano, R., Bando, T., Ishikawa, R., Giono, G., Tsuneta, S., Nakayama, S., and Tajima, T., "Development of a Precise Polarization Modulator for UV Spectropolarimetry," *Sol. Phys.* **290**, 3081–3088 (Oct 2015).

[10] Giono, G., Katsukawa, Y., Ishikawa, R., Narukage, N., Kano, R., Kubo, M., Ishikawa, S., Bando, T., Hara, H., Suematsu, Y., Winebarger, A., Kobayashi, K., Auchère, F., and Trujillo Bueno, J., "Optical alignment of the Chromospheric Lyman-Alpha Spectro-Polarimeter using sophisticated methods to minimize activities under vacuum," *Proc. SPIE* **9905**, 99053D (July 2016).

[11] Giono, G., Ishikawa, R., Narukage, N., Kano, R., Katsukawa, Y., Kubo, M., Ishikawa, S., Bando, T., Hara, H., Suematsu, Y., Winebarger, A., Kobayashi, K., Auchère, F., and Trujillo Bueno, J., "Polarization Calibration of the Chromospheric Lyman-Alpha SpectroPolarimeter for a 0.1 % Polarization Sensitivity in the VUV Range. Part I: Pre-flight Calibration," *Sol. Phys.* **291**, 3831–3867 (Dec 2016).

[12] Narukage, N., Kubo, M., Ishikawa, R., Ishikawa, S.-n., Katsukawa, Y., Kobiki, T., Giono, G., Kano, R., Bando, T., Tsuneta, S., Auchère, F., Kobayashi, K., Winebarger, A., McCandless, J., Chen, J., and Choi, J., "High-Reflectivity Coatings for a Vacuum Ultraviolet Spectropolarimeter," *Sol. Phys.* **292**, 40 (Mar. 2017).

[13] Ishikawa, S.-n., Shimizu, T., Kano, R., Bando, T., Ishikawa, R., Giono, G., Beabout, D. L., Beabout, B. L., Nakayama, S., and Tajima, T., "In-flight performance of the polarization modulator in the CLASP rocket experiment," *Proc. SPIE* **9905**, 99052U (July 2016).

[14] Giono, G., Ishikawa, R., Narukage, N., Kano, R., Katsukawa, Y., Kubo, M., Ishikawa, S., Bando, T., Hara, H., Suematsu, Y., Winebarger, A., Kobayashi, K., Auchère, F., Trujillo Bueno, J., Tsuneta, S., Shimizu, T., Sakao, T., Cirtain, J., Champey, P., Asensio Ramos, A., Štěpán, J., Belluzzi, L., Manso Sainz, R., De Pontieu, B., Ichimoto, K., Carlsson, M., Casini, R., and Goto, M., "Polarization Calibration of the Chromospheric Lyman-Alpha SpectroPolarimeter for a 0.1% Polarization Sensitivity in the VUV Range. Part II: In-Flight Calibration," *Sol. Phys.* **292**, 57 (Apr 2017).

[15] Kano, R., Trujillo Bueno, J., Winebarger, A., Auchère, F., Narukage, N., Ishikawa, R., Kobayashi, K., Bando, T., Katsukawa, Y., Kubo, M., Ishikawa, S., Giono, G., Hara, H., Suematsu, Y., Shimizu, T., Sakao, T., Tsuneta, S., Ichimoto, K., Goto, M., Belluzzi, L., Štěpán, J., Asensio Ramos, A., Manso Sainz, R., Champey, P., Cirtain, J., De Pontieu, B., Casini, R., and Carlsson, M., "Discovery of Scattering Polarization in the Hydrogen Lyα Line of the Solar Disk Radiation," *Astrophys. J. Lett.* **839**, L10 (Apr. 2017).

[16] Ishikawa, R., Trujillo Bueno, J., Uitenbroek, H., Kubo, M., Tsuneta, S., Goto, M., Kano, R., Narukage, N., Bando, T., Katsukawa, Y., Ishikawa, S., Giono, G., Suematsu, Y., Hara, H., Shimizu, T., Sakao, T., Winebarger, A., Kobayashi, K., Cirtain, J., Champey, P., Auchère, F., Štěpán, J., Belluzzi, L., Asensio Ramos, A., Manso Sainz, R., De Pontieu, B., Ichimoto, K., Carlsson, M., and Casini, R., "Indication of the Hanle Effect by Comparing the Scattering Polarization Observed by CLASP in the Lyα and Si III 120.65 nm Lines," *Astrophys. J.* **841**, 31 (May 2017).

[17] Landi Degl'Innocenti, E. and Landolfi, M., [*Polarization in Spectral Lines*], vol. 307, Springer Netherlands (2004).

[18] Štěpán, J., Trujillo Bueno, J., Belluzzi, L., Asensio Ramos, A., Manso Sainz, R., del Pino Alemán, T., Casini, R., Kano, R., Winebarger, A., Auchère, F., Ishikawa, R., Narukage, N., Kobayashi, K., Bando, T., Katsukawa, Y., Kubo, M., Ishikawa, S., Giono, G., Hara, H., Suematsu, Y., Shimizu, T., Sakao, T., Tsuneta, S., Ichimoto, K., Cirtain, J., Champey, P., De Pontieu, B., and Carlsson, M., "A Statistical Inference Method for Interpreting the CLASP Observations," *Astrophys. J.* **865**, 48 (Sept. 2018).

[19] Trujillo Bueno, J., Štěpán, J., Belluzzi, L., Asensio Ramos, A., Manso Sainz, R., del Pino Alemán, T., Casini, R., Ishikawa, R., Kano, R., Winebarger, A., Auchère, F., Narukage, N., Kobayashi, K., Bando, T., Katsukawa, Y., Kubo, M., Ishikawa, S., Giono, G., Hara, H., Suematsu, Y., Shimizu, T., Sakao, T., Tsuneta, S., Ichimoto, K., Cirtain, J., Champey, P., De Pontieu, B., and Carlsson, M., "CLASP Constraints on the Magnetization and Geometrical Complexity of the Chromosphere-Corona Transition Region," *Astrophys. J.* **866**, L15 (Oct 2018).

[20] Narukage, N., McKenzie, D. E., Ishikawa, R., Trujillo-Bueno, J., De Pontieu, B., Kubo, M., Ishikawa, S.-n., Kano, R., Suematsu, Y., Yoshida, M., Rachmeler, L. A., Kobayashi, K., Cirtain, J. W., Winebarger, A. R., Asensio Ramos, A., del Pino Aleman, T., Štěpán, J., Belluzzi, L., Larruquert, J. I., Auchère, F., Leenaarts, J., and Carlsson, M. J. L., "Chromospheric LAyer SpectroPolarimeter (CLASP2)," *Proc. SPIE* **9905**, 990508 (July 2016).

[21] Alsina Ballester, E., Belluzzi, L., and Trujillo Bueno, J., "The Magnetic Sensitivity of the Mg II k Line to the Joint Action of Hanle, Zeeman, and Magneto-optical Effects," *Astrophys. J.* **831**, L15 (Nov 2016).

[22] del Pino Alemán, T., Casini, R., and Manso Sainz, R., "Magnetic Diagnostics of the Solar Chromosphere with the Mg II h-k Lines," *Astrophys. J.* **830**, L24 (Oct 2016).

[23] Ishikawa, R., Uitenbroek, H., Goto, M., Iida, Y., and Tsuneta, S., "Influence of the Atmospheric Model on Hanle Diagnostics," *Sol. Phys.* **293**, 74 (Apr. 2018).

[24] Yoshida, M., Song, D., Ishikawa, R., Kano, R., Katsukawa, Y., Suematsu, Y., Narukage, N., Kubo, M., Shinoda, K., Okamoto, T. J., McKenzie, D. E., Rachmeler, L. A., Auchère, F., and Trujillo Bueno, J., "Wavefront error measurements and alignment of CLASP2 telescope with a dual-band pass cold mirror coated primary mirror," *Proc. SPIE* **10699**, 1069930 (July 2018).

[25] Kubo, M., Katsukawa, Y., Suematsu, Y., Kano, R., Band o, T., Narukage, N., Ishikawa, R., Hara, H., Giono, G., Tsuneta, S., Ishikawa, S., Shimizu, T., Sakao, T., Winebarger, A., Kobayashi, K., Cirtain, J., Champey, P., Auchère, F., Trujillo Bueno, J., Asensio Ramos, A., Štěpán, J., Belluzzi, L., Manso Sainz, R., De Pontieu, B., Ichimoto, K., Carlsson, M., Casini, R., and Goto, M., "Discovery of Ubiquitous Fast-Propagating Intensity Disturbances by the Chromospheric Lyman Alpha Spectropolarimeter (CLASP)," *Astrophys. J.* **832**, 141 (Dec. 2016).

[26] Berger, T., Mudge, J., Holmes, B., Searcy, P., Wuelser, J. P., Lemen, J., and Title, A., "Design and fabrication of the near-ultraviolet birefringent Solc filter for the NASA IRIS solar physics mission," *Proc. SPIE* **8486**, 84860G (Oct. 2012).

[27] Song, D., Ishikawa, R., Kano, R., Yoshida, M., Tsuzuki, T., Uraguchi, F., Shinoda, K., Hara, H., Okamoto, T. J., Auchère, F., McKenzie, D. E., Rachmeler, L. A., and Trujillo Bueno, J., "Optical alignment of the high-precision UV spectro-polarimeter (CLASP2)," *Proc. SPIE* **10699**, 106992W (July 2018).